Integrative and Comparative Biology

Integrative and Comparative Biology, volume 62, number 3, pp. 625–640
https://doi.org/10.1093/icb/icac110

Society for Integrative and Comparative Biology

SYMPOSIUM

History-Dependent Deformations of Rat Vaginas under Inflation

Justin Dubik[*], Alfonsina Tartaglione[†], Kristin S. Miller[‡], David A. Dillard[§] and Raffaella De Vita[*,1]

[*]STRETCH Lab, Department of Biomedical Engineering and Mechanics, Virginia Tech, 330A Kelly Hall, 325 Stanger Street, Blacksburg, VA 24061, USA; [†]Department of Mathematics and Physics, Università degli Studi della Campania "Luigi Vanvitelli", Viale Abramo Lincoln 5, Caserta, CE 81100, Italy; [‡]Department of Biomedical Engineering, Tulane University, 531 Lindy Boggs, New Orleans, LA 70118, USA; [§]Department of Biomedical Engineering and Mechanics, Virginia Tech, 219A Norris Hall, 495 Old Turner Street, Blacksburg, VA 24061, USA

From the symposium "Morphology and evolution of female copulatory morphology in Amniotes" presented at the annual meeting of the Society for Integrative and Comparative Biology virtual annual meeting, January 3–February 28, 2022.

[1]E-mail: devita@vt.edu

Synopsis The vagina is a highly inhomogeneous, anisotropic, and viscoelastic organ that undergoes significant deformations *in vivo*. The mechanical attributes of this organ facilitate important physiological functions during menstruation, intercourse, and birthing. Despite the crucial mechanical role that the vagina plays within the female reproductive system, the deformations that the organ can sustain over time under constant pressure, in both the longitudinal direction (LD) and circumferential direction (CD), have not been fully characterized. This experimental study focuses on quantifying the creep properties of the vagina via *ex vivo* inflation testing using the rat as an animal model. Toward this end, rat vaginas were subjected to three consecutively increasing constant luminal pressures (28, 55, and 83 kPa) using a custom-built experimental setup and the resulting inhomogeneous deformations were measured using the digital image correlation (DIC) method. The vagina was found to deform significantly more in the CD than the LD at any constant pressure, suggesting that the organ primarily adapts to constant pressures by significantly changing the diameter rather that the length. The change in deformation over time was significantly higher during the first inflation test at a constant pressure of 28 kPa than during the second and third inflation tests at constant pressures of 55 and 83 kPa, respectively. The findings of this study on the mechanical behavior of the vagina could serve to advance our limited knowledge about the physiology and pathophysiology of this important reproductive organ.

Introduction

The United States has one of the highest Cesarean section (C-section) rates: 31.8% of all live births were C-sections in 2020 (Osterman et al. 2022). Although C-sections are necessary and lifesaving, they can place both mothers and babies at increased health risks when performed without medical reasons. Mothers are more likely to incur complications during subsequent pregnancies and babies are more likely to suffer from asthma (Keag et al. 2018). On the other hand, several studies have suggested that C-sections protect women from pelvic floor disorders such as urinary incontinence and prolapse compared to vaginal birth. Women who deliver by C-section have about half the risk of developing pelvic floor disorders later in life compared with women who have a spontaneous vaginal birth (Wu et al. 2014). The biomechanical process of childbirth has not been sufficiently studied (Grimm 2021), and a better understanding of the deformations that the reproductive system experiences during labor may improve maternal health, establishing universal standards for the recommendation of C-sections and post-natal care guidelines to reduce incidence of pelvic floor disorders.

Fundamental research on the biomechanical properties of the vagina is crucial since this organ undergoes astonishing remodeling to accommodate the full passage of a baby during the second stage of labor. Characterizing this complex remodeling process *in vivo* is impossible due to ethical reasons, and thus *ex vivo* experimental studies are often conducted to under-

Advance Access publication July 4, 2022

stand the mechanical function of the vagina. The vagina has a very heterogeneous micro-structure being made of three to four layers (Krstic 2013) and being compositionally different in the proximal (closer to the cervix), mid, and distal (closer to the introitus) regions (Rynkevic et al. 2017; Ulrich et al. 2014a, 2014b; Huntington et al. 2022). The variation in the content and organization of the primary components of the vagina (collagen, smooth muscle, and elastin fibers) are likely responsible for the mechanical behavior of this organ. The vaginas of many mammals, including rats, mice, and ewes, have many organizational and microstructural similarities, and for this reason mechanical studies frequently make use of animal models to understand the function of this organ and the roles of its micro-structural components (McCracken et al. 2021).

Research on the mechanical properties of the vagina has primarily focused on characterizing the *ex vivo* elastic properties of the organ (Baah-Dwomoh et al. 2016; Huntington et al. 2020). Uniaxial tensile tests have been conducted on both human cadaveric tissue (Rubod et al. 2008, 2012; Jean-Charles et al. 2010; Chantereau et al. 2014) and animal tissue (Rubod et al. 2007; Rahn et al. 2008; Martins et al. 2010; Knight et al. 2016; Orbach et al. 2019), demonstrating nonlinearity in the elastic response of the vagina. Recently, biaxial tests have become more prevalent to quantify the anisotropy of the tissue, capturing differences in mechanical behavior between the two primary anatomical directions of the vagina: the longitudinal direction (LD) and the circumferential direction (CD). These tests better replicate *in vivo* physiological loading conditions. Planar biaxial testing has been used to study the passive elastic and tear propagation properties of the swine vagina (McGuire et al. 2019a), as well as the active elastic properties of the rat vagina subjected to electrical and chemical stimulation (Huntington et al. 2019, 2021). To evaluate the mechanical properties of the vagina in its original tubular structure, researchers have further performed inflation tests and measured the mechanical response of the vaginal tissue of rats (Alperin et al. 2010; McGuire et al. 2019b) and mice (Robison et al. 2017; Clark et al. 2019). In these biaxial studies, the vagina was found to exhibit its characteristic nonlinear behavior, as well as both passive and active anisotropy (Clark et al. 2019; McGuire et al. 2019b; Huntington et al. 2019, 2021).

Knowledge of the elastic behavior of the vagina is insufficient to fully elucidate the role of this organ during parturition. The second stage of labor in humans can last upwards of 1 h (WHO 2018), during which the vagina is mechanically stressed due to the rising pressures from the uterus and the baby. With such a long duration of loading, the viscoelastic properties, or time-dependent mechanical properties, of the vagina become particularly important for delivery. Additionally, it has been shown that the vagina undergoes microstructural alterations throughout pregnancy to facilitate delivery [in the rat (Daucher et al. 2007)], although these changes and the resulting mechanical changes have not been fully described. Specifically, the viscoelastic behavior of the vagina must be studied under a variety of loading conditions (e.g., uniaxial tests, planar biaxial tests, and inflation tests) and protocols (e.g., hysteresis, creep, and relaxation) and during gestation, including prior to it, to fully describe the organ's biomechanical role during parturition.

To date, the viscoelasticity of the vagina has only been described by a few investigators. Phenomena like hysteresis, stress relaxation, and creep that are typical of viscoelastic materials have been observed in vaginal tissue from mice, ewes, dolphins, swine, and humans (Peña et al. 2010, 2011; Ulrich et al. 2014b; Orbach et al. 2019; Pack et al. 2020; Clark-Patterson et al. 2021). Uniaxial tensile tests of ewe vaginal tissue have demonstrated hysteresis behavior (i.e., different load–deformation curves during loading and unloading), followed by some permanent deformation (Ulrich et al. 2014b). This viscoelastic behavior has been also reported for dolphin and human vaginal tissue subjected to loading and unloading uniaxial tensile tests (Peña et al. 2011; Orbach et al. 2019). By adopting similar testing methods, human vaginal tissue has been found to exhibit stress relaxation (i.e., decrease in load over time under constant deformation) (Peña et al. 2010). Planar biaxial tests of swine vaginal tissue have also provided data on the stress relaxation, showing a more significant decrease in stress over time in the LD than in the CD (Pack et al. 2020). Most recently, the creep behavior, the increase in deformation over time under constant load, of the murine vagina has been quantified in the CD via inflation-extension tests (Clark-Patterson et al. 2021). However, to the authors' knowledge, no mechanical data exist regarding the biaxial creep behavior of the vagina in both the LD and CD.

This study focuses on characterizing the history-dependent deformations of the vagina using the rat as an animal model. Rats are selected due to their anatomical, microstructural, and genetic similarity to humans, as well as their common use in biomedical research (McCracken et al. 2021). Deformations are induced using a custom-built inflation setup which is designed to pressurize vaginal specimens while allowing their free extension in the LD. Vaginal specimens are subjected to three different constant pressures over the same time interval to reveal the effect of pressure history on the deformations and curvatures of the vagina. Given the complex heterogeneous micro-structure of the vagina, the digital image correlation (DIC) method is used to

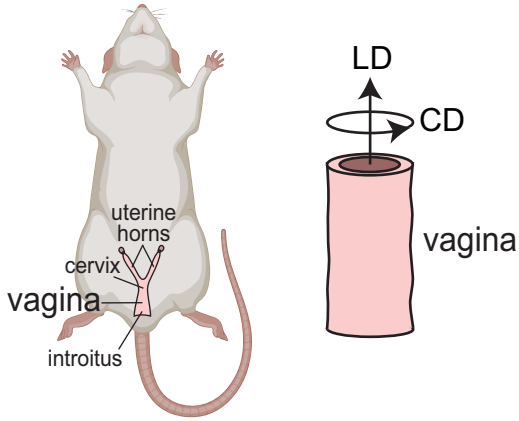

Fig. 1 Schematic of the rat vagina showing the longitudinal direction (LD) and circumferential direction (CD).

measure local variation in strains as well as local variation in curvatures and explore differences between the LD and CD. Together strain and curvature measurements provide a complete picture of how much the rat vagina expands and how much the shape of this organ changes over time under constant pressure. The findings of this study have the potential to cast new light on the function of this organ during copulation and parturition, ultimately having long-term health benefits to mothers.

Methods

Specimen preparation

This study was conducted with the approval of the Institutional Animal Care and Use Committee at Virginia Tech. Twenty virgin rats between nine and ten weeks of age were sacrificed, then frozen at -20°C. Freezing has been found to have minimal effects on the mechanical response of vaginal tissue (Rubod et al. 2007). For testing, the rats were thawed over 1–2 days at 4°C before the vaginal tracts were isolated via dissection (Fig. 1). Specifically, the whole vaginal canal was dissected from introitus to cervix, and excess tissue removed with the exception of the urethra. The urethra could not be safely removed without substantial risk of damage to the vaginal canal. Following dissection, the vaginal specimens were kept hydrated by spraying 1× phosphate-buffered saline (PBS) (pH 7.4, Fisher Scientific, USA) periodically on the specimens until testing. Images of the proximal cross-sections of the vaginas were collected under microscope using a CMOS camera (Thorlabs Inc., Newton, NJ, USA). The inner radius and thickness for each specimen were measured using the path and line drawing tools of ImageJ (NIH, Bethesda, MD, USA), respectively. Their values are presented as mean ± standard deviation (SD) in Table 1.

Specimens were subsequently mounted onto 6- and 8-gauge concentric needles as depicted in Fig. 2A and described by McGuire et al. (2019b), such that the upper 8-gauge needle was allowed to freely extend vertically relative to the fixed 6-gauge lower needle as the vagina was inflated. The vaginal canal was mounted with the introitus on the fixed lower needle. The vaginal canal was secured over O-rings using fishing line and cyanoacrylate adhesive, and the ends were further secured using Teflon tape (Fig. 2A). The upper needle assembly weighed ∼0.026 N. Once mounted, the axial length of each specimen was measured via digital calipers (accuracy: ±0.1 mm, Mitutoyo Absolute Low Force Calipers Series 573, Kawasaki, Japan) and was used together with the inner radius to estimate the inner volume of the specimen. The mean (±SD) value of the inner volume is reported in Table 1. Specimens were then dyed with a 1% methylene blue solution (Fisher Science Education, Nazareth, PA, USA) and speckled with white spray paint (Rust-Oleum, Vernon Hills, IL, USA) to create a high contrast speckle pattern for non-contract strain measurement during testing (Lionello et al. 2014).

Experimental protocol

Testing was performed using a custom-built inflation set-up, with the components schematically shown in Fig. 2B, at room temperature. After being mounted on needles, specimens were immersed in an acrylic tank filled with 8 L 1× PBS. The specimens were connected via plastic tubing to a pressure transducer (max capacity: 345 kPa, accuracy ±0.03 %, Omega Engineering, Norwalk, CT, USA) and a computer-controlled syringe pump (accuracy: ±1%, NE 1000, New Era Pump Systems, Inc., Farmingdale, NY, USA) that infused PBS into the specimens during testing. Readings from the pressure transducer were interpreted and recorded via a myDAQ (accuracy: ±0.5%, +20 mV, National Instruments, Austin, TX, USA) and a custom MATLAB script (R2018a, Mathworks, Natick, MA, USA).

Specimens were pre-loaded to a luminal pressure of 1.4 kPa. The configuration of the specimens at this specific pressure was used as reference configuration since this pressure was sufficient to support the weight of the upper needle assembly (McGuire et al. 2019b). Specimens were then preconditioned from the reference configuration to 150% of their initial volume and back to the reference configuration at a flow rate of 4.7 mL min^{-1} for 20 cycles. Preconditioning was performed to obtain a steady and repeatable mechanical response of the vaginal tissue before measuring mechanical properties. The specimens were then unloaded and allowed to recover for 600 s, and then pre-loaded to 1.4 kPa once again.

Table 1 Mean (±SD) inner radius, thickness, length, and inner volume of the vaginal specimens ($n = 20$).

	Inner radius (mm)	Thickness (mm)	Length (mm)	Inner volume (mm^3)
Mean	2.55	0.39	10.66	253.12
SD	0.04	0.08	1.29	31.54

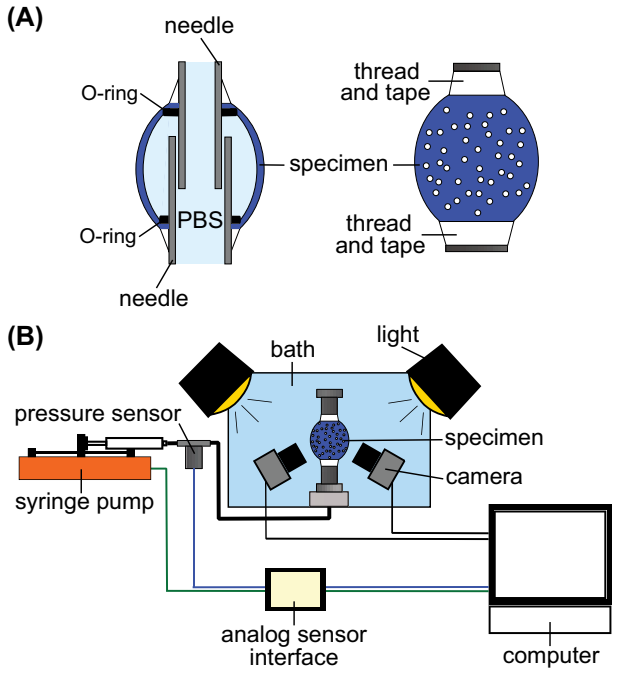

Fig. 2 Schematic of **(A)** transverse cross-section of coaxial needles that hold a rat vaginal tissue specimen and vaginal tissue specimen speckled for non-contact strain measurement and **(B)** custom-made inflation setup.

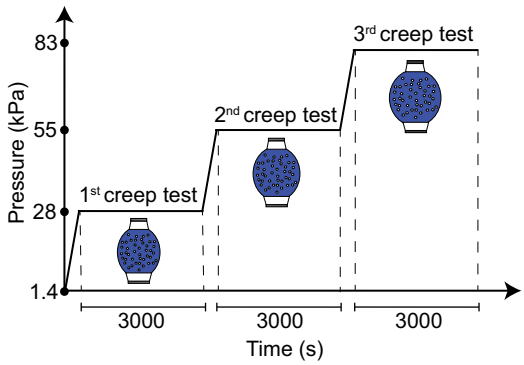

Fig. 3 Experimental protocol used to test rat vaginal specimens consisting of three pre-creep ramp tests, where the pressure is increased from the reference configuration (1.4 kPa) to 28 kPa, from 28 to 55 kPa, and from 55 to 83 kPa, and three creep tests, where the pressure is kept constant at 28, 55, and 83 kPa over a time interval of 3000 s.

Figure 3 depicts the experimental protocol after preconditioning. The protocol consists of three pre-creep tests up to luminal pressures of 28, 55, and 83 kPa, each with subsequent creep tests and no recovery between pre-creep and creep tests. Specifically, the specimens were inflated at a constant volume rate of 0.7 mL min^{-1} until they reached a luminal pressure of 28 kPa during the first pre-creep tests. They were then kept at 28 kPa luminal pressure for 3000 s for the subsequent first creep tests. This process was repeated for the second and third pre-creep and creep tests, to luminal pressures of 55 and 83 kPa, respectively with no return to the reference state. The pre-creep inflation rate of 0.7 mL min^{-1} was determined through preliminary testing, as higher rates such as those used by McGuire et al. (2019b) would frequently to pressures higher than the target pressures. In order to keep the pressure constant during creep tests, the vaginal specimens were periodically re-inflated at a rate of 0.1 mL min^{-1} by means of a closed-loop analog control sensor interface (Ana-Box^{TM} Model ADPT-ANABOX-11, New Era Pump Systems, Inc., Farmingdale, NY, USA) and a voltage multiplier connected to the pressure transducer (Fig. 2B). The values of the three applied pressures, 28, 55, and 83 kPa, which correspond with imperial values for 4, 8, and 12 psi, were chosen to be lower than the mean pressure that caused rupture of vaginal specimens in previous studies (McGuire et al. 2019b).

During pre-creep, high-resolution images (2448 × 2048 pixels) were captured at 2 Hz via two CMOS cameras (Basler ace acA2440-75 um, Basler, Inc., Exton, PA, USA) equipped with c-mount lenses (Xenoplan 2.8/50, Schneider Optics Inc., Hauppauge, NY). During creep, when pressure was nominally maintained constant, the image capture rate was reduced to 0.2 Hz. The vaginal canal was oriented with the dorsal side facing the cameras throughout testing to avoid imaging the urethra. Non-contact strain measurements were performed with a 3D DIC system (strain resolution >10 $\mu\epsilon$, Vic-3D 9, Correlated Solutions, Columbia, SC, USA). The CMOS cameras were calibrated for DIC by use of a through-light calibration grid (4-in-1 9 × 9 dot Calibration Target, Correlated Solutions, Columbia, SC, USA) before testing. Maps of the local normal Lagrangian strains and curvatures in the LD and CD across the surface of each specimen were obtained using the DIC system.

Data analysis

Normal stresses in the LD and CD were calculated by assuming the inflated vaginal canal acts as a thick-walled pressure vessel. Using the cross-sectional dimensions measured as described earlier and the pressures recorded from the pressure transducer, the normal nominal stresses in the LD and CD, σ_{zz} and $\sigma_{\theta\theta}$ respectively, are calculated by

$$\sigma_{zz} = \frac{Pr_i^2}{2r_i t + t^2} - \frac{F}{\pi\left(r_o^2 - r_i^2\right)},$$
$$\sigma_{\theta\theta} = \frac{2Pr_i^2}{2r_i t + t^2}, \quad (1)$$

where P is the luminal pressure, F is the weight of the upper needle assembly, and r_i, r_o, and t are the inner radius, outer radius, and thickness of the vaginal canal, respectively.

To compute the strain for each specimen from the map of local normal Lagrangian strains, a small circular region of diameter <1 mm was selected on the dorsal side of the vagina (i.e., the side exposed to the cameras), away from the clamped ends. From this small circular region, the average normal Lagrangian strains in the LD and CD across the region were calculated for every image recorded during testing. These average normal Lagrangian strains were taken as the representative strains for that specimen, and are hereby referred to simply as the strains in the LD and CD. The representative curvatures for each specimen were calculated from the same circular region, and are likewise referred to simply as the curvatures in the LD and CD.

Strain and curvature data in the LD and CD were computed throughout testing, both during pre-creep and creep tests, for each specimen. The change in strain during a creep test was calculated by subtracting the initial strain at the beginning of the creep test from the strain data at any subsequent time during that creep test. Therefore, for each specimen, there were six data sets for the change in strain (or curvature) throughout creep: one in the LD and one in the CD for each of the three creep tests at 28, 55, and 83 kPa.

To compare the initial and final creep rates during testing between each of the creep tests, primary creep was defined as the creep occuring during the first 500 s while secondary creep was defined as the creep occuring after 1000 s. For all creep tests in each direction, the primary creep rate was then calculated by the slope of the linear regression of the change in strain versus time for the first 500 s of creep. The secondary creep rate was calculated by the slope of the linear regression of the change in strain versus time from $t = 1000$ s to the end of the creep test.

Statistical analysis

Of the twenty specimens tested, only data from fourteen specimens were analyzed due to rupture or negative strain in the LD during creep for six specimens. On the group of fourteen, statistical comparisons were performed using SPSS statistical software (SPSS version 27, IBM, Armonk, NY, USA). A two-way factorial repeated-measures ANOVA was used to compare the difference in strains at the beginning of the creep tests, with factors being the order of creep test (first, second, and third creep tests) and anatomical direction (LD and CD). The strains at the beginning of the first creep test were not normally distributed as determined by Ryan–Joiner test ($P = 0.016$ for strains in the LD and $P = 0.043$ for strains in the CD), with one outlier for the strains in the LD as determined by Grubbs' test. For the second and third creep tests, the initial strains were normally distributed as determined by Ryan–Joiner test. A $\log_{10}(x)$ transformation was performed to normalize the initial strain values (x).

The changes in strain during creep in each direction were analyzed at four time points into each test: $t = 250$, 500, 1000, and 3000 s. A three-way factorial repeated-measures ANOVA was used to compare the effect of anatomical orientation (LD and CD), order of creep test (first, second, and third creep tests), and time during creep (250, 500, 1000, and 3000 s) on the change in strain during creep. The changes in strain in the CD at $t = 250$ s and $t = 1000$ s into the first creep test were not normally distributed as determined by Ryan–Joiner test, with one outlier as determined by Grubbs' test at $t = 250$ s. A $\log_{10}(x + 0.01)$ transformation was performed to normalize the data, as there were nonpositive strain values (x) that could not be subjected to a $\log_{10}(x)$ transformation.

The creep rates were compared via three-way factorial repeated-measures ANOVA, with anatomical direction (LD versus CD), order of creep test (first, second, and third creep tests), and creep phase (primary versus secondary) as factors. The creep rates were all normally distributed as determined by Ryan–Joiner test.

In all cases where the N-way factorial repeated measures ANOVA were performed, the following procedure was followed. Greenhouse-Geisser corrections were applied as appropriate when assumptions of sphericity were violated. If a significant two-way interaction was observed, simple main effects were assessed via one-way repeated measures ANOVA tests. If no significant two-way interaction was found between two of the N factors, then the data were grouped together based on one of the two factors and main effects were assessed. When significant main effects or significant simple main effects were found, post hoc analysis was performed with

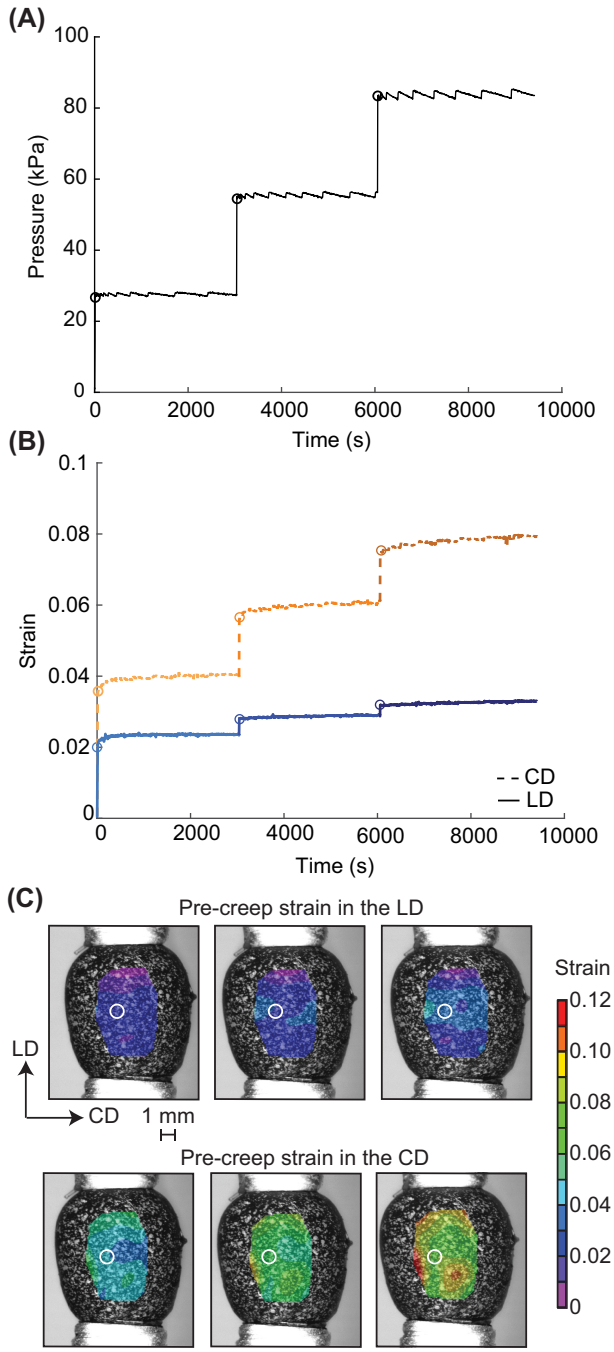

Fig. 4 (A) Pressure versus time data and **(B)** corresponding average (normal Lagrangian) strains in the LD and CD for one representative specimen during both the three pre-creep and creep tests. **(C)** Local (normal Lagrangian) strains in the LD and CD for this specimen at the beginning of the first, second, and third creep tests. White circles represent the regions of interest from which the representative strains were measured.

Bonferroni correction for pairwise comparisons. No significant three-way interactions were found.

Statistical significance was set at $P < 0.05$. In all cases where data transformations were performed, the transformation resulted in normalized data sets by Ryan–Joiner test, and statistical comparisons were performed on both the original and transformed data sets. In all cases, statistically significant differences were found on both original and transformed data. Therefore, results are reported for statistical comparisons as performed on the original data. All data are presented as mean ± standard error of the mean (SEM), unless noted otherwise.

Results

Both pressure and strain data versus time recorded throughout the entire experimental protocol (schematically shown in Fig. 3) for one representative vaginal specimen are presented in Fig. 4. The duration of the pre-creep tests were on the order of 10 s, which is less than 1% of the 3000 s duration of the creep tests. It can be seen that the pressure increased sharply during the three pre-creep tests, and was relatively constant during the three creep tests, with periodic sawtooth increases and decreases due to the pressure control system (Fig. 4A). The strain in both the LD and CD increased quickly during the pre-creep tests, and increased slowly during the creep tests as shown for the representative specimen in Fig. 4B. Moreover, throughout testing, the strain in the CD remained greater than the strain in the LD. The strain fields in both the LD and CD are shown in Fig. 4C at the beginning of each of the three creep tests for the representative specimen. The local strains varied across the surface of each specimen, with the strain fields of the representative specimen reaching values as high as 0.12 in some regions and values <0.01 in others.

The pressure–strain data in the LD and CD for all specimens during the pre-creep tests are presented in Fig. 5. There was variation in the mechanical behavior between the vaginal specimens. During the first pre-creep up to 28 kPa, the strain increased nonlinearly with the pressure (Figs. 5A and B). The variation among specimens was more pronounced in these initial nonlinear pressure–strain curves, as the extent of the toe region of these curves differed. One specimen in particular (data in green in Figs. 5A and B) was extremely compliant in both the LD and CD, and another one (data in yellow in Fig. 5B) was extremely compliant in just the CD. Beyond this pressure and after the first creep tests, the pressure–strain response was linear in both the LD and CD (Figs. 5C and F). In each direction, the slopes were visually similar between the second and third pre-creep tests. For the second pre-creep test, all the strain data in the LD varied from 0.016 to 0.050 and all the strain data in the CD varied from 0.022 to 0.072. For the third pre-creep test, all the strain data in the LD varied from 0.023 to 0.057, while all the strain data in the CD varied from 0.034 to 0.090. In other words, in each

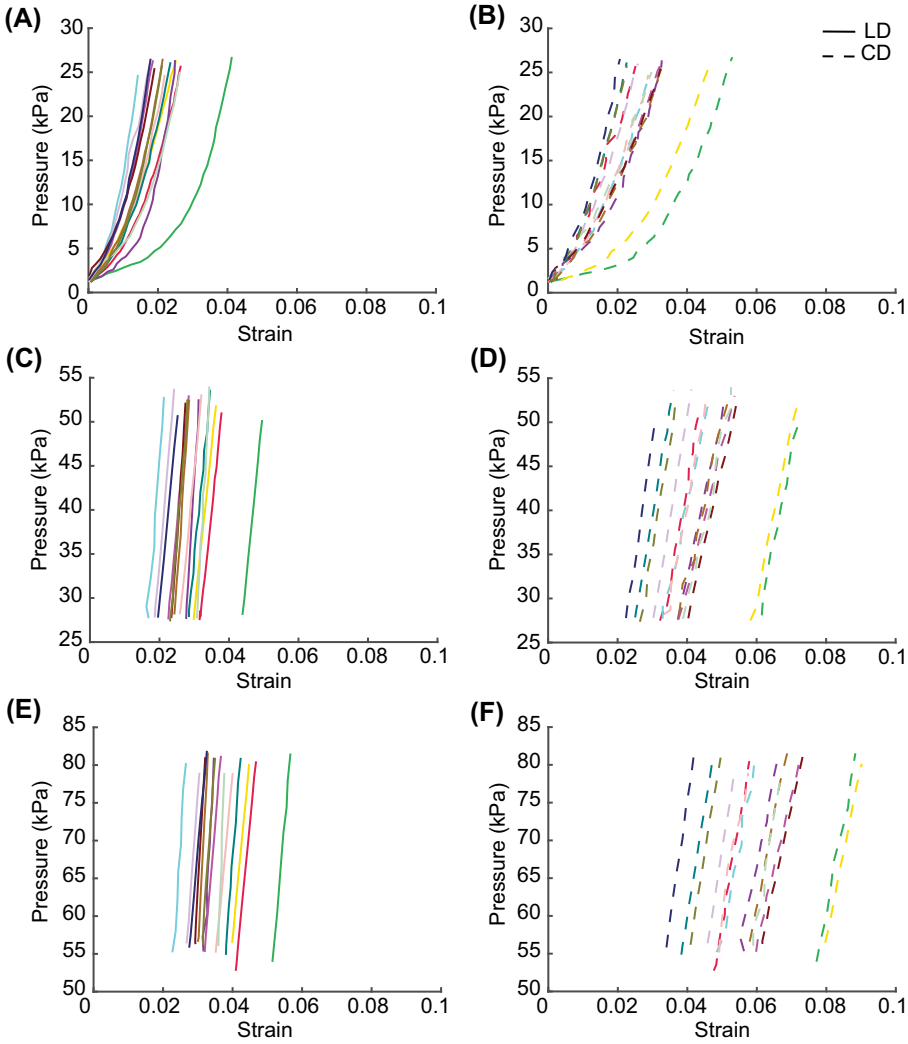

Fig. 5 Pressure versus strain data in the LD (solid lines) and CD (dashed lines) during the **(A** and **B)** first pre-creep tests, **(C** and **D)** second pre-creep tests, and **(E** and **F)** third pre-creep tests for all specimens ($n = 14$). Data collected from the same specimen are represented using the same color.

direction, the strain intervals were relatively similar between the second and third pre-creep tests, although such intervals were greater in the CD than in the LD.

For each specimen, the pressure–curvature data in the LD and CD during pre-creep are reported in Fig. 6. For most specimens, there was very little change in curvature as the pressure increased. In the LD, the curvature stayed almost constant (Figs. 6A, C, and E), while the curvature in the CD slightly decreased (Figs. 6B, D, and F). Such decrease in curvature was greater in the CD during the first pre-creep, but varied across the tested specimens (Figs. 6B).

The applied stresses and resulting initial strains (mean ±SEM) in the LD and CD at the beginning of the three creep tests (or, equivalently, at the end of the pre-creep tests) are reported in Table 2. At the beginning of each creep test, the stresses were greater in the CD than the LD and they increased in both directions as the pressure increased to reach the constant values of the first, second, and third creep tests. This is expected since the stresses were computed using equation (1). By two-way ANOVA, there was a significant interaction between the anatomical direction and the order of creep test on the initial strains ($P < 0.001$). By ANOVA, the mean strains in the CD were significantly higher than the mean strains in the LD at the beginning of each of the creep tests ($P < 0.001$). From test to test, the pairwise comparisons of the initial strains before the first, second, and third creep revealed significant changes in mean strain in both the LD and CD between creep tests ($P < 0.001$).

The mean (±SEM) change in strain over time observed during creep at all three pressures (28, 55, and 83 kPa) are presented in Fig. 7. In both the LD and CD,

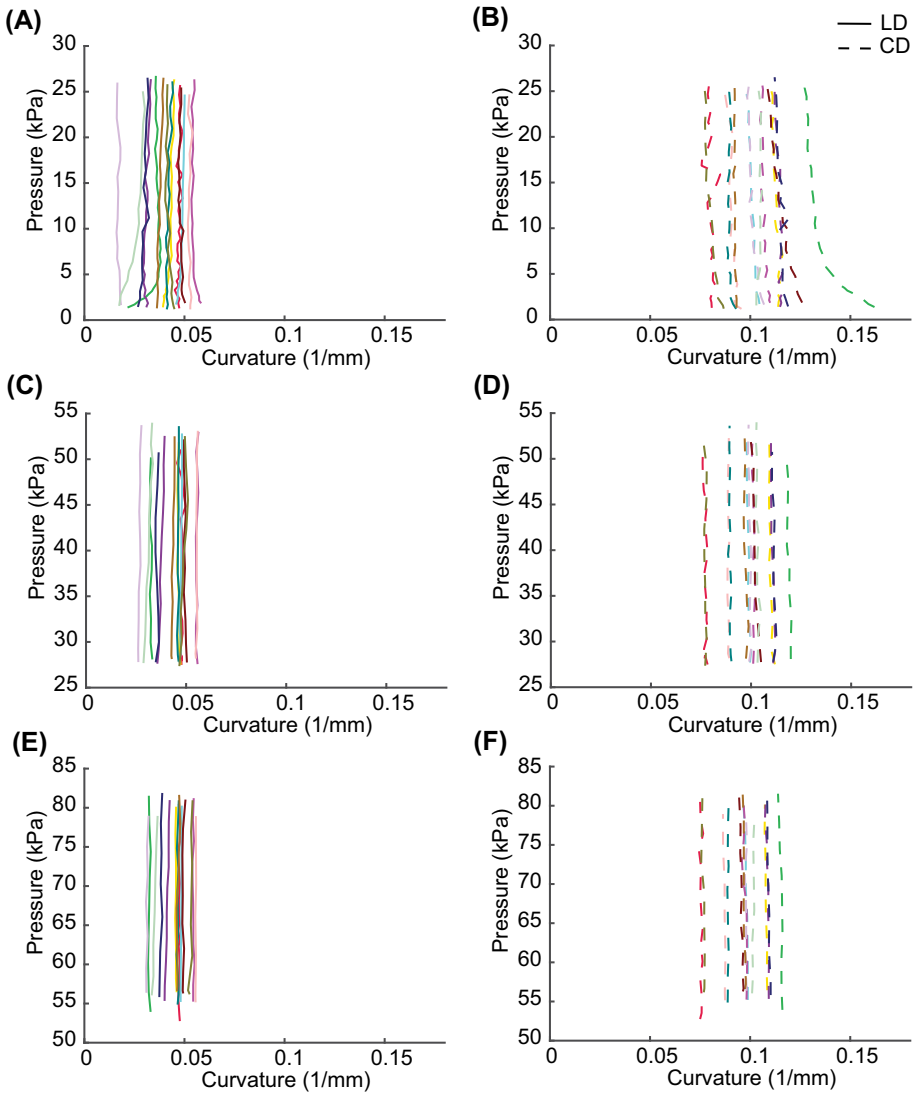

Fig. 6 Pressure versus curvature in the LD (solid lines) and CD (dashed lines) during the **(A** and **B)** first pre-creep tests, **(C** and **D)** second pre-creep tests, and **(E** and **F)** third pre-creep tests for all specimens ($n = 14$). Data collected from the same specimen are represented using the same color.

Table 2 Mean (±SEM) stresses and strains at the beginning of the three creep tests (or, equivalently, at the end of the pre-creep tests).

P (kPa)	σ_{zz} (kPa)	$\sigma_{\theta\theta}$ (kPa)	E_{zz}	$E_{\theta\theta}$
28	78.6 ± 3.8	164.8 ± 8.0	0.023 ± 0.002	0.032 ± 0.002
55	161.1 ± 8.0	329.8 ± 16.4	0.032 ± 0.002	0.050 ± 0.003
83	245.6 ± 11.9	498.8 ± 24.3	0.038 ± 0.002	0.065 ± 0.004

σ_{zz}: stress in the LD, $\sigma_{\theta\theta}$: stress in the CD, E_{zz}: strain in the LD, and $E_{\theta\theta}$: strain in the CD ($n = 14$).

and at all pressures, the mean strain increased quickly during primary creep (up to 500 s). During secondary creep (after 1000 s), the mean strain increased much more slowly and the creep rate remained relatively constant. The total change in mean strain decreased from the first creep test to the second or third creep test in both directions. Figure 7 shows that the vaginal tissues consistently strained more in the CD than in the LD during creep through all creep tests.

The mean (±SEM) change in strain at several time points ($t = 250$, 500, 1000, and 3000 s) are plotted in Fig. 8. The mean strain increased at these time points (i.e., the change in strain was always positive) in both directions during all creep tests ($n = 14$), and the vaginal

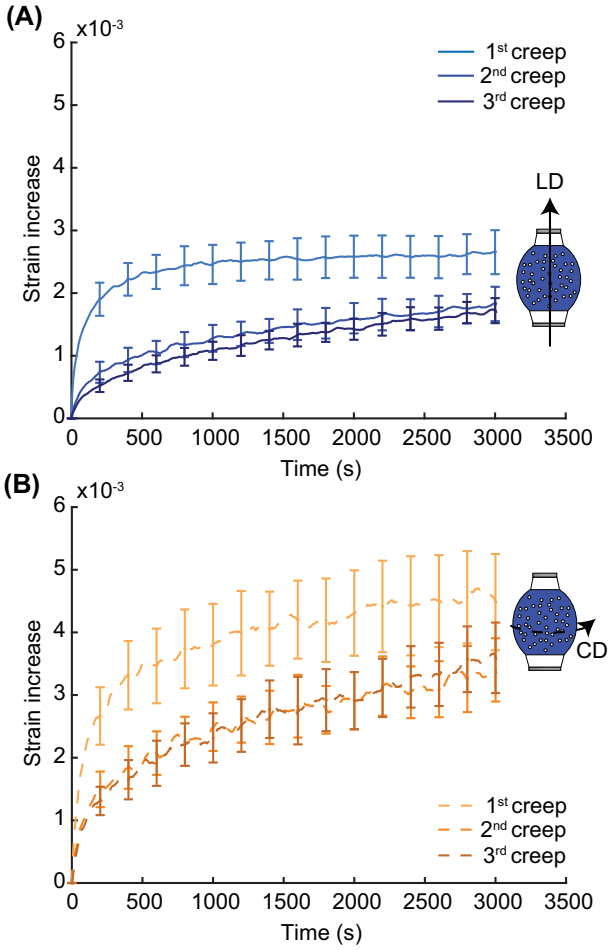

Fig. 7 Mean (±SEM) increase in strain versus time during the first, second, and third creep tests in the **(A)** LD and **(B)** CD ($n = 14$).

tissue strained more in the CD than the LD. Note this excludes the three specimens which underwent a large decrease in strain in the LD during the first creep test. By factorial ANOVA, there was a significant interaction between anatomical direction and time during creep on the mean change in strain ($P = 0.008$). After grouping all the data collected during the first, second, and third creep tests together, there was a significant difference in the mean change in strain between the LD and CD, at all time points ($P < 0.001$). Similarly, time was found to be a significant factor on the mean change in strain in both directions ($P < 0.001$). By pairwise comparisons, there was a significant difference between the change in strain at all time points ($t = 250$, 500, 1000, and 3000 s), in either the LD or the CD ($P < 0.001$). By factorial ANOVA, there was also a significant interaction between the time and the order of creep test on the mean change in strain ($P < 0.001$). When grouping the data in the LD and CD together, the order of creep test was a significant factor at all time points ($P < 0.001$). By pairwise comparisons, the first creep test was significantly different from the second and third creep tests ($P \leq 0.028$). The second and third creep tests were not significantly different from each other ($P \geq 0.265$). Moreover, time was a significant factor through all creep tests ($P < 0.001$). By pairwise comparisons, there was a significant difference in the mean change in strain between all four time points, at each of the three creep tests ($P \leq 0.005$).

The mean (±SEM) primary and secondary creep rates for the first, second, and third creep tests are reported in Fig. 9. In both the LD and CD, one can visually observe from Fig. 9 that the primary creep rates decreased from the first creep test to the second creep test but remained almost unchanged between the second and third creep tests (Fig. 9A). Conversely, the secondary creep rates visually appear to have increased from the first to the second and from the second to the third creep test in both the LD and CD (Fig. 9B). By factorial ANOVA, there was a significant interaction between the anatomical direction (LD and CD) and creep phase (primary and secondary) ($P = 0.006$). After grouping the data collected in the first, second, and third creep tests together, the primary creep rates were significantly greater than secondary creep rates in each direction ($P < 0.001$). Similarly, creep rates were significantly higher in the CD than the LD, during both primary and secondary creep ($P < 0.001$). By factorial ANOVA, there was also a significant interaction between the creep phase and the order of creep test on the creep rates ($P < 0.001$). After grouping the data in the LD and CD together, the primary creep rates were significantly greater than the secondary creep rates at each of the three creep tests ($P < 0.001$). The order of creep test was a significant factor for both the primary and secondary creep rates ($P < 0.001$). By pairwise comparisons, the primary creep rates were significantly different between the first creep test and the second creep test, as well as between the first creep test and the third creep test ($P < 0.001$). The primary creep rates during the second and third creep tests were not significantly different from one another ($P = 1.000$). Conversely, the pairwise comparisons on the secondary creep rates revealed a significant difference between all three creep tests ($P \leq 0.005$).

The mean (±SEM) curvature data in the LD and CD over time during each of the three creep tests are plotted in Fig. 10. The mean (±SEM) curvatures in the LD and CD at $t = 0$ s and $t = 3000$ s in each of the three creep tests are reported in Table 3. The mean curvatures in both the LD and CD appeared to change, slightly increasing in the LD and decreasing in the CD over time, for each of the three creep tests. In the LD, this change was more pronounced during the first creep test, with much of the change occurring specifically in the first few hundred seconds of creep (Fig. 10A).

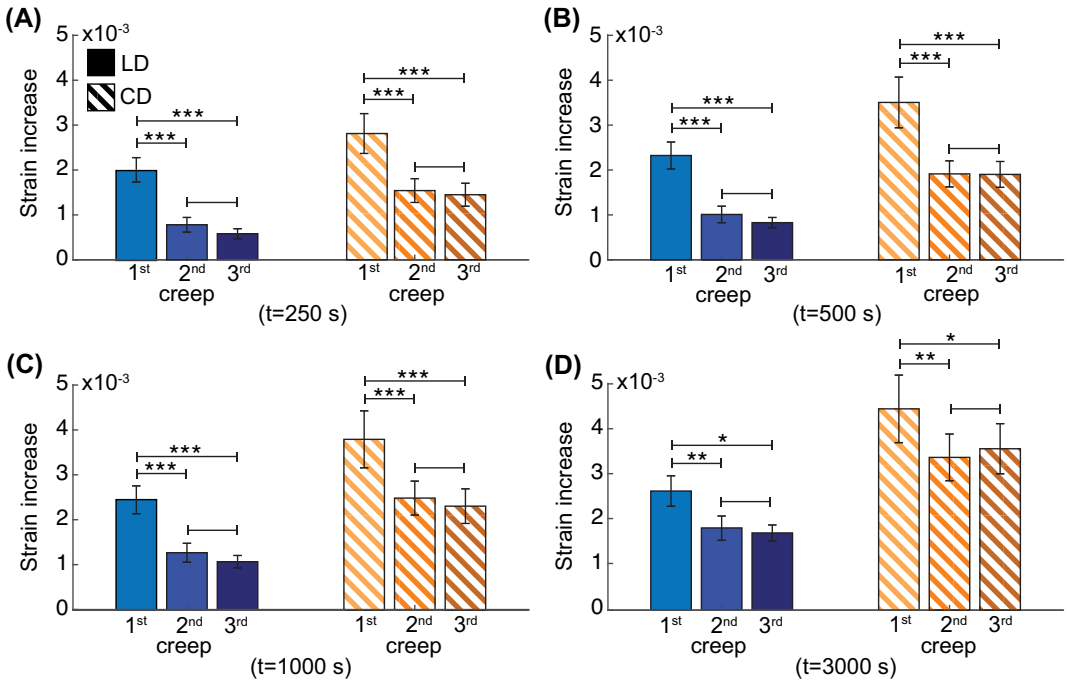

Fig. 8 Mean (±SEM) increase in strain in the LD and CD for the first, second, and third creep tests at **(A)** $t = 250$ s, **(B)** $t = 500$ s, **(C)** $t = 1000$ s, and **(D)** $t = 3000$ s. The change in strain at all four times were significantly different from one another for all three creep tests ($P < 0.01$). The change in strain in the CD was higher than the LD at all times ($P < 0.001$). $^{*}P < 0.05$, $^{**}P < 0.01$, $^{***}P < 0.001$.

In the CD, the decrease in curvature was more pronounced during the second and third creep tests (Fig. 10B).

Discussion

To the authors' knowledge, this is the first experimental study to characterize the history-dependent biaxial deformations of rat vaginal tissue under increasing and constant pressures using the DIC technique. The vaginal canal underwent inhomogeneous deformations through inflation testing, experiencing greater strains in the CD than the LD during both pre-creep and creep tests. The local variations in strain can be attributed to variations in the architecture of the main microstructural components (e.g., smooth muscle and collagen fibers) of the organ. For example, areas of lower strain in the LD may be attributable to the presence of more fibers oriented toward the LD (McGuire et al. 2021; Huntington et al. 2022).

During the first pre-creep tests, we reported a nonlinear increase in strain with increasing pressure (Figs. 5A and B) and a linear relationship between pressure and strain after the first creep tests, during the second and third pre-creep tests (Figs. 5C, D, E, and F). Variation in the mechanical response across specimens was consistent with previous studies of vaginal tissue, particularly our previous inflation to rupture study (McGuire et al. 2019b). During the second and third pre-creep tests, the slopes of the pressure–strain response of the specimens were remarkably consistent with one another. This change in the pre-creep pressure–strain response from nonlinear during the first pre-creep to linear during the second and third pre-creep likely resulted from the re-orientation and un-crimping of collagen fibers when the specimens were subjected to the first pre-creep tests and the subsequent first creep tests. Quantitatively, we did not observe a notable difference in apparent stiffness of the rat vaginal tissue between the LD and CD during pre-creep (Table 2). Specifically, by the end of testing, both the stress and strain in the LD were approximately half of their respective values in the CD. The lack of differences between the elastic pre-creep response in the two directions in our study may be due in part to the lower applied pressures with respect to our previous study. Within these smaller pressures/stresses, it is possible that the fibrous components of the vaginal tissue remained fully or partially crimped, and thus the ground substance in which the fibers were embedded dominated the overall mechanical behavior. Furthermore, the 3000 s long interval between the first and second pre-creep tests, when the tissue was held at 28 kPa, possibly allowed straightening of the collagen fibers at lower stresses than those applied during quasi-static tests. Such straightening might have altered the mechanical response of the specimens in the subsequent pre-creep tests.

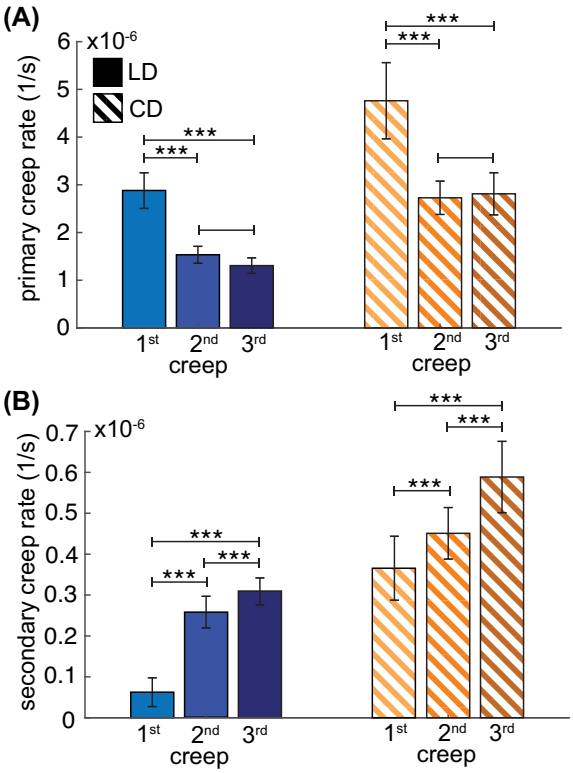

Fig. 9 (A) Mean (±SEM) primary creep rates and **(B)** mean (±SEM) secondary creep rates in the LD and CD for the first, second, and third creep tests ($n = 14$). The primary creep rates were significantly different from the secondary creep rates for all creep tests in both directions ($P < 0.001$). The creep rates in the CD were greater than the creep rates in the LD through both primary and secondary creep ($P < 0.001$). $^{*}P < 0.05$, $^{**}P < 0.01$, $^{***}P < 0.001$.

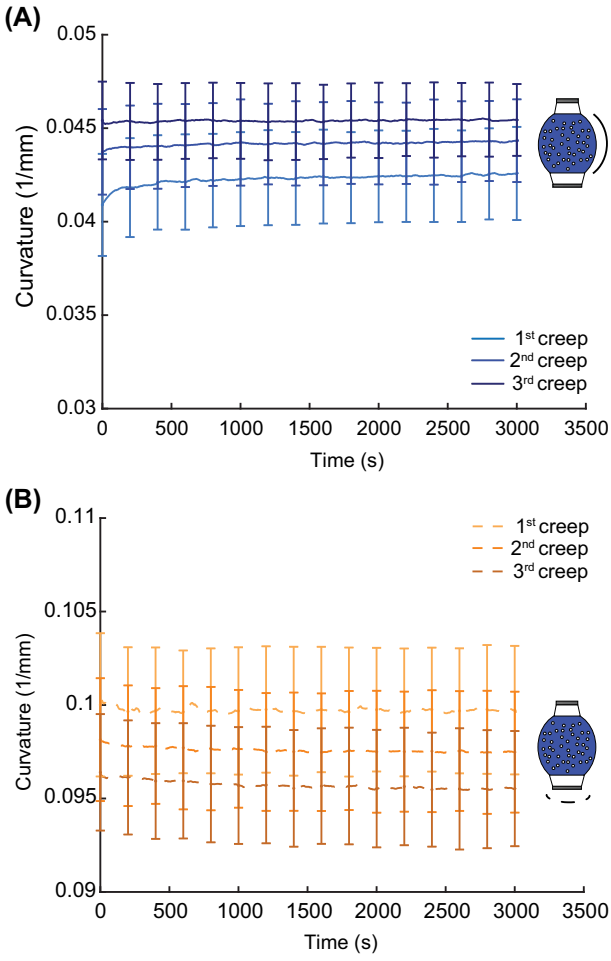

Fig. 10 Mean (±SEM) curvature versus time in the **(A)** LD and **(B)** CD during the first, second, and third creep tests ($n = 14$).

After 3000 s of creep, we reported a mean (± S.E.M.) change in strain of 0.0045 ± 0.0008 in the CD for the first creep test (Figs. 7 and 8). Much of this change in strain occurred early into creep: after only 100 s, we recorded an increase of 0.0022 ± 0.0004 in the same direction during the first creep test. This is comparable with the results of Clark-Patterson et al. (2021), who after 100 s of creep, reported similar increases in strain in the CD ranging from 0.0028 ± 0.0003 to 0.0041 ± 0.0003. They conducted four inflation creep tests of wildtype/haploinsufficient mice using balloon catheters at target pressures of 0.67, 0.93, 1.33, and 2.00 kPa, each conducted for 100 s with 1000 s allowed for recovery between creep tests, at fixed axial lengths ranging between ±4% of the physiologic axial length. We notably report a lower amount of creep strain despite the fact that we inflated to higher stresses during our first creep test than Clark-Patterson et al. did during any of their creep tests (Clark-Patterson et al. 2021). This difference in results can be explained by difference in chosen animal models, testing apparatus, and methods of strain measurement. Specifically, Clark-Patterson et al. used wildtype/haploinsufficient mice for their study of vaginal tissue, which in addition to being much smaller than the Sprague-Dawley rats we used, may have differing microstructure [e.g., a thicker epithelial layer than the rat vagina (McCracken et al. 2021)]. Furthermore, while they fixed the axial length and estimated strain from the diameter of the vagina, we allowed for free-extension of the organ in the LD and measured the local strains across the dorsal side via DIC.

We performed three consecutive creep tests, each 3000 s long, without recovery to examine the effects of loading history on the time-dependent deformation behavior of the vagina, and found that the amount of strain decreased from the first creep test to the second and third (Figs. 7 and 8). Comparatively, when allowing time for recovery between creep tests, Clark Patterson et al. (2021) reported an increase in creep strain with increasing pressure in vaginal tissue under inflation. The reduction in creep strain we observed during consecutive creep tests appears to be a result of a

Table 3 Mean (± SEM) curvatures (mm^{-1}) at $t = 0$ s and $t = 3000$ s in each of the three creep tests, in the LD and CD ($n = 14$).

	Curvature in the LD		Curvature in the CD	
	$t = 0$ s	$t = 3000$ s	$t = 0$ s	$t = 3000$ s
First creep test	0.0409 ± 0.0027	0.0426 ± 0.0025	0.1000 ± 0.0038	0.0997 ± 0.0034
Second creep test	0.0437 ± 0.0023	0.0443 ± 0.0022	0.0981 ± 0.0033	0.0972 ± 0.0032
Third creep test	0.0454 ± 0.0021	0.0455 ± 0.0019	0.0964 ± 0.0031	0.0955 ± 0.0031

change in the initial creep behavior. The primary creep rates in the LD and CD decreased from the first creep test to the second and third (Fig. 9A). Conversely, the secondary creep rates in both directions increased from test to test (Fig. 9B), and it is possible that if the creep tests had a longer duration than 3000 s, the changes in strain during the second and third creep tests may have surpassed the change in strain during the first creep test. We note that the definitions of primary and secondary creep adopted in this study were based on qualitative observations that the rate of change in strain during creep tended to decrease dramatically within the first 1000 s, and the exact limits chosen for defining the timescales of primary creep and secondary creep were arbitrary. Ultimately, we choose to use these definitions as they provide a useful shorthand for comparing the creep rates at the beginning and end of each of the three creep tests.

We speculate that the differing behavior of the vaginal tissue during primary creep and secondary creep is possibly controlled by two distinct mechanisms: water exudation/collagen fiber uncrimping and collagen fiber–matrix interaction/collagen interfibrillar sliding. During primary creep, some water may have exuded out of the vaginal tissue, as suggested by Baah-Dwomoh and De Vita (2017) in their study of the creep properties of swine cardinal ligaments at multiple repeated biaxial loads. As water left the tissue, the fibers within the tissue may have re-arranged themselves giving rise to the initial nonlinearity of the strain versus time behavior (i.e., the primary creep behavior). If this was the case, primary creep may have been limited in consecutive creep tests, as much of the water was squeezed out during the first creep and, without recovery, the tissues did not have time to reabsorb water. Consequently, the fibers did not have sufficient time to re-arrange themselves and regain some undulation. In studies that included recovery time between creep tests, some water might have been reabsorbed by the tissue, allowing for similar primary creep behavior in subsequent tests. However, Baah-Dwomoh and De Vita (2017) noted that the first creep test always resulted in greater normalized strain than the subsequent tests, even after recovery, irrespective of the magnitude of the applied biaxial loads, suggesting that complete water reabsorption may take a very long time.

Alternatively or concomitantly, primary creep might have been determined by collagen fiber uncrimping. It has been shown that collagen fibers within the vagina straighten and reorient as the tissue is loaded to stiffen and strengthen the organ (Clark et al. 2019; McGuire et al. 2021). While collagen fiber reorientation has been shown to not be time-dependent in ligaments (Purslow et al. 1998), we know very little about the time dependency of crimping/uncrimping of collagen fibers. Primary creep may be less significant in consecutive creep tests with no recovery because many of the collagen fibers are already straightened during the first creep test. During recovery time between creep test, the fibers may regain the undulation so that primary creep behavior does not change in subsequent creep tests. The secondary creep behavior of vaginal tissue could be governed by fiber–matrix interaction and sliding of the fibrils within the matrix as suggested by a few investigators (Purslow et al. 1998; Thornton et al. 2001). Such sliding would be unchanged as water re-enters the tissue during recovery but, without recovery, sliding could be further favored in subsequent creep tests. Moreover, the secondary creep rate could continue to increase in consecutive creep tests, as the fibers need not be undulated to slide within the matrix at a relatively stable rate. Futher research is needed to investigate the role of the vaginal microstructure during creep. Particularly, mechanical tests that utilize DIC methods for in-plane strain measurements with other optical techniques, such as polarized light microscopy for imaging of collagen fibers or optical coherence tomography for detecting out-of-plane microstructural changes, may serve to shed light on the deformation mechanisms during creep.

We reported greater strains in the CD than the LD throughout all creep tests (Fig. 7). However, this by itself does not indicate anisotropy in the creep response, as the vaginal specimens in their tubular configuration experienced less stress in the LD than the CD. Moreover, our factorial ANOVA of the change in strain during creep with the order of the creep test and anatomical direction as factors revealed no significant interaction between such factors. This indicates that the deforma-

tion history of multiple creep tests had a relatively similar effect in the LD and CD. However, as discussed earlier the lack of anisotropy in the pre-creep response was likely resulting from low stresses applied to the tissue. The same may hold true for investigating anisotropy in the creep response, particularly since the first creep test was conducted at very low stresses. Other forms of biaxial creep testing, such as planar biaxial testing, may be better suited for elucidating potential anisotropy in the viscoelastic response of the vagina.

In our custom-built inflation setup, the pressure was controlled via a closed-loop analog control sensor interface, which was used in tandem with a custom-made variable voltage multiplier attached to the pressure transducer. This control system allowed us to keep the pressure within ±1.5 kPa of the selected pressure values during creep tests. These fluctuations in the target pressures often led to periodic sawtooth patterns in the pressure versus time data, as can be seen in Fig. 4A. Pressure fluctuations would inevitably have an effect on the strains of the specimens during creep (as can be noted in Fig. 7). Rather than using a commercial pressure regulator, we preferred to use the variable voltage multiplier system in our setup since it allowed for easy and quick switching between nominally/approximately constant creep pressures for consecutive creep tests. Future studies of creep resulting from inflation to one pressure could consider implementing a pressure regulator to reduce pressure fluctuations over time.

Of the twenty specimens tested, three failed due to rupture during the third creep test. No observations were made during specimen preparation and testing that would indicate a predisposition to failure of these specimens over others. Figure 11A depicts one of these specimens at the moment of failure, at which point the luminal pressure dropped from 82.7 to 0.3 kPa in a matter of seconds. The resulting tears on each of the three specimens were small and difficult to locate post-experiment, but each occurred outside the view of the cameras, on the ventral or the lateral side of the vaginal canal as depicted in Fig. 11A. It is worth noting that McGuire et al. (2019b) found that the ventral wall was the predominant region of tear formation in their study of inflation to rupture of vaginal tissue, and Rubod et al. (2012) reported that cadaveric vaginal tissue from the posterior region (dorsal region in rats) was significantly stronger than tissue from the anterior region (ventral region for rats). Collectively, these findings may suggest that the ventral vagina is mechanically different from the dorsal vagina in the rat, and therefore one must use the panoramic DIC technique proposed by Genovese et al. (2013) to quantify possible regional differences in the deformations of the organ.

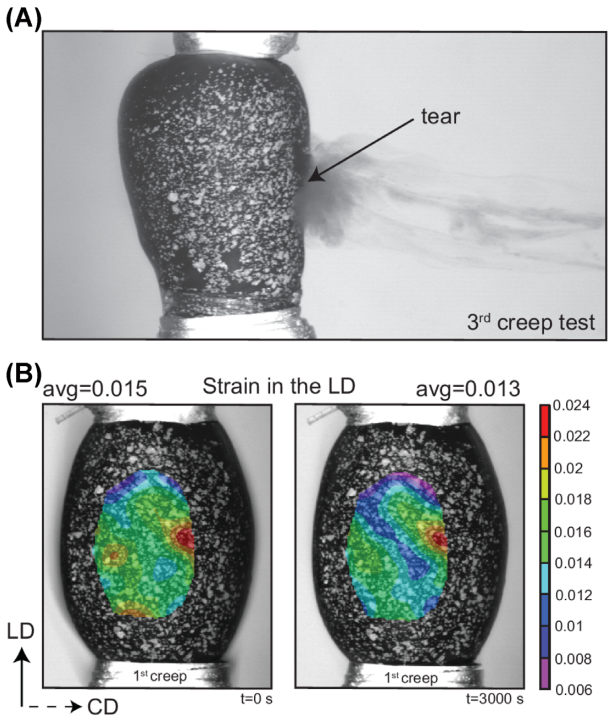

Fig. 11 (A) Specimen rupturing during the third creep. The specimen was inflated to a luminal pressure of 82.7 kPa at the moment it ruptured. **(B)** Maps of strains in the LD at $t = 0$ s and $t = 3000$ s for a vaginal specimen experiencing a decrease in strain (instead of the usual increase in strain) over time during creep. The average strains (across the specimen) are reported on the top of each image at $t = 0$ s and $t = 3000$ s.

The results of three additional specimens were not reported, as they exhibited a large decrease in strain in the LD during the first creep test. Figure 11B depicts the strain fields in the LD for one of these specimens at the beginning and end of the first creep test. Across the specimen, the local strains in the LD decreased from the beginning to the end of the first creep test. All three specimens ultimately experienced an increase in strain in the LD during the third creep test. Negative strain during creep may be due to strong coupling between anatomical loading directions: as the tissue was loaded biaxially, it compressed in one direction to become more compliant in the other direction. It is worth noting that all these three specimens exhibited a positive change in strain during creep in the CD through all three tests. Additionally, these specimens exhibited unusually stiff stress–strain behavior in the LD compared to the other specimens of this study.

Consistently with our previous inflation study (McGuire et al. 2019b), we reported higher curvatures in the CD than the LD throughout pre-creep inflation testing (Fig. 6). These higher curvatures in the CD provide affirmation that the vagina is accurately assumed to behave as a cylindrical pressure vessel under

inflation during these experiments. During pre-creep, there was a greater change in curvature with pressure in the CD than the LD, with most of the change in curvature occurring during the first pre-creep, as the organ was first inflated (Figs. 6A and B). The curvature also underwent more consistent change in the CD than the LD during creep, particularly in the second and third creep tests (Fig. 10, Table 3). This suggests that the rat vagina under pressure appeared to expand in the CD, with little change in shape in the LD. These findings agree with the physiological role that the organ plays in copulation and parturition, when it needs to increase in size primarily along its circumference.

In this study, we characterize the history-dependent mechanical properties of rat vaginal specimens that had been previously frozen. Although a previous study by Rubod et al. (2007) suggested that freezing ewe vaginal specimens does not alter uniaxial tensile properties, it is unclear whether their finding can be extended to biaxial inflation tests on rat vaginal specimens, or to the viscoelastic behavior of the vagina. Certainly, when using frozen specimens, the mechanical contribution of smooth muscle fibers, which are abundant in the muscularis of the organ and are aligned toward the LD (Huntington et al. 2022), is not considered. Planar biaxial experiments in our lab have demonstrated that KCl-induced contractions of the rat vagina cause strains up to 15%, and these strains are significantly larger in the LD than the CD (Huntington et al. 2019, 2021). The strains measured during pre-creep and creep were higher in the CD during inflation, but it is possible that, when the tissue is fresh and able to contract, the strains are comparable in the LD and CD or even higher in the LD. Future studies in our lab will investigate the interplay between the active and viscoelastic properties of the vagina.

Conclusions

This study presents the first investigation of the creep behavior of vaginal tissue in both the LD and CD, using free-extension inflation testing to apply three incrementally increasing constant pressures and measuring the strain fields using the DIC method. The tissue deformed more in the CD than the LD under any of the applied constant pressures. In both anatomical directions, vaginal specimens exhibited a higher increase in strain during the first creep test than during the second or third creep tests. This was associated with a reduction in the primary creep rate and an increase in the secondary creep rate after the first creep test. In other words, these findings suggest that the vagina under incremental constant loads over time, such as during delivery or copulation, stretches more during the first applied load than during subsequent loads. Specifically, stretching occurs quickly immediately after the load is applied and more slowly later on as load is sustained. Moreover, the diameter of the vagina increases more than the length under constant load. This dependence of creep behavior and creep rates on the loading history is likely attributed to micro-structural changes that occur within the tissue over time under pressure. The results of this study provide a significant insight into the long-term viscoelastic behavior of vaginal tissue under biaxial loading, which is vital to improve the medical treatment of parous women in the United States.

Author contributions statement

R.D., D.D., and J.D. conceived the experiments; J.D. conducted the experiments; J.D., D.D., and R.D. analyzed the results; R.D., J.D., D.D., A.T., and K.M. wrote and reviewed the manuscript.

Acknowledgments

The authors would like to thank the Jarome Lab at Virginia Tech for providing rats for testing, Dr. McGuire and Mr. Adam Vossenberg for their assistance with inflation testing, and Ms. Finnley Rogers for her aid in statistical analysis.

Competing interests

The authors declare that they have no known competing financial interests or personal relationships that could have appeared to influence the work reported in this paper.

Funding

This work was supported by funds from the National Science Foundation [grant numbers NSF # 1929731 and # 2053851).

Data availability

The data that support the findings of this study are available from the corresponding author, R.D., upon reasonable request.

References

Alperin M, Feola A, Duerr R, Moalli P, Abramowitch S. 2010. Pregnancy-and delivery-induced biomechanical changes in rat vagina persist postpartum. Int Urogynecol J 21: 1169–74.

Baah-Dwomoh A, De Vita R. 2017. Effects of repeated biaxial loads on the creep properties of cardinal ligaments. J Mech Behav Biomed 74: 128–41.

Baah-Dwomoh A, McGuire J, Tan T, De Vita R. 2016. Mechanical properties of female reproductive organs and supporting

connective tissues: a review of the current state of knowledge. Appl Mech Rev 68: 060801.
Chantereau P, Brieu M, Kammal M, Farthmann J, Gabriel B, Cosson M. 2014. Mechanical properties of pelvic soft tissue of young women and impact of aging. Int Urogynecol J 25: 1547–53.
Clark GL, Pokutta-Paskaleva AP, Lawrence DJ, Lindsey SH, Desrosiers L, Knoepp LR, Bayer CL, Gleason RL, Miller KS. 2019. Smooth muscle regional contribution to vaginal wall function. Interface Focus 9: 20190025.
Clark-Patterson GL, McGuire JA, Desrosiers L, Knoepp LR, De Vita R, Miller KS. 2021. Investigation of murine vaginal creep response to altered mechanical loads. J Biomech Eng 143: 121008.
Daucher JA, Clark KA, Stolz DB, Meyn LA, Moalli PA. 2007. Adaptations of the rat vagina in pregnancy to accommodate delivery. Obstet Gynecol 109: 128–35.
Genovese K, Lee YU, Lee AY, Humphrey JD. 2013. An improved panoramic digital image correlation method for vascular strain analysis and material characterization. J Mech Behav Biomed 27: 132–42.
Grimm MJ. 2021. Forces involved with labor and delivery—a biomechanical perspective. Ann Biomed Eng 49: 1819–35.
Huntington A, Rizzuto E, Abramowitch S, Del Prete Z, De Vita R. 2019. Anisotropy of the passive and active rat vagina under biaxial loading. Ann Biomed Eng 47: 272–81.
Huntington A, Donaldson K, De Vita R. 2020. Contractile properties of vaginal tissue. J Biomech Eng 142: 080801.
Huntington A, Abramowitch SD, Moalli PA, De Vita R. 2021. Strains induced in the vagina by smooth muscle contractions. Acta Biomater 129: 178–87.
Huntington AJ, Udayasuryan B, Du P, Verbridge SS, Abramowitch SD, De Vita R. 2022. Smooth muscle organization and nerves in the rat vagina: a first look using tissue clearing and immunolabeling. Ann Biomed Eng 50: 440–51.
Jean-Charles C, Rubod C, Brieu M, Boukerrou M, Fasel J, Cosson M. 2010. Biomechanical properties of prolapsed or non-prolapsed vaginal tissue: impact on genital prolapse surgery. Int Urogynecol J 21: 1535–8.
Keag OE, Norman JE, Stock SJ. 2018. Long-term risks and benefits associated with cesarean delivery for mother, baby, and subsequent pregnancies: systematic review and meta-analysis. PLoS Med 15: e1002494.
Knight KM, Moalli PA, Nolfi A, Palcsey S, Barone WR, Abramowitch SD. 2016. Impact of parity on ewe vaginal mechanical properties relative to the nonhuman primate and rodent. Int Urogynecol J 27: 1255–63.
Krstic RV. 2013. Human microscopic anatomy: an atlas for students of medicine and biology. New York (NY): Springer Science & Business Media.
Lionello G, Sirieix C, Baleani M. 2014. An effective procedure to create a speckle pattern on biological soft tissue for digital image correlation measurements. J Mech Behav Biomed 39: 1–8.
McCracken JM, Calderon GA, Robinson AJ, Sullivan CN, Cosgriff-Hernandez E, Hakim JCE. 2021. Animal models and alternatives in vaginal research: a comparative review. Reprod Sci 28: 1759–73.
McGuire JA, Abramowitch SD, Maiti S, De Vita R. 2019a. Swine vagina under planar biaxial loads: an investigation of large deformations and tears. J Biomech Eng 141: 041003.
McGuire JA, Crandall CL, Abramowitch SD, De Vita R. 2019b. Inflation and rupture of vaginal tissue. Interface Focus 9: 20190029.
McGuire JA, Monclova JL, Coariti ACS, Stine CA, Toussaint KC, Munson JM, Dillard DA, De Vita R. 2021. Tear propagation in vaginal tissue under inflation. Acta Biomater 127: 193–204.
Martins PALS, Peña E, Calvo B, Doblaré M, Mascarenhas T, Natal Jorge R, Ferreira A. 2010. Prediction of nonlinear elastic behaviour of vaginal tissue: experimental results and model formulation. Comput Meth Biomech Biomed Eng 13: 327–37.
Orbach DN, Rattan S, Hogan M, Crosby AJ, Brennan PLR. 2019. Biomechanical properties of female dolphin reproductive tissue. Acta Biomater 86: 117–24.
Organization WH et al. 2018. Intrapartum care for a positive childbirth experience. Geneva: World Health Organization. p. 150.
Osterman MJK, Hamilton BE, Martin JA, Driscoll AK, Valenzuela CP. 2022. Births: final data for 2020. Natl Vital Stat Rep 70: 1–50.
Pack E, Dubik J, Snyder W, Simon A, Clark S, De Vita R. 2020. Biaxial stress relaxation of vaginal tissue in pubertal gilts. J Biomech Eng 142: 031002.
Peña E, Calvo B, Martínez MA, Martins PALS, Mascarenhas T, Jorge RMN, Ferreira A, Doblaré M. 2010. Experimental study and constitutive modeling of the viscoelastic mechanical properties of the human prolapsed vaginal tissue. Biomech Model Mechanobiol 9: 35–44.
Peña E, Martins P, Mascarenhas T, Jorge RMN, Ferreira A, Doblaré M, Calvo B. 2011. Mechanical characterization of the softening behavior of human vaginal tissue. J Mech Behav Biomed 4: 275–83.
Purslow PP, Wess TJ, Hukins DW. 1998. Collagen orientation and molecular spacing during creep and stress-relaxation in soft connective tissues. J Exp Biol 201: 135–42.
Rahn DD, Ruff MD, Brown SA, Tibbals HF, Word RA. 2008. Biomechanical properties of the vaginal wall: effect of pregnancy, elastic fiber deficiency, and pelvic organ prolapse. Am J Obstet Gynecol 198: 590–e1.
Robison KM, Conway CK, Desrosiers L, Knoepp LR, Miller KS. 2017. Biaxial mechanical assessment of the murine vaginal wall using extension–inflation testing. J Biomech Eng 139: 104504.
Rubod C, Boukerrou M, Brieu M, Dubois P, Cosson M. 2007. Biomechanical properties of vaginal tissue. part 1: new experimental protocol. J Urol 178: 320–5.
Rubod C, Boukerrou M, Brieu M, Jean-Charles C, Dubois P, Cosson M. 2008. Biomechanical properties of vaginal tissue: preliminary results. Int Urogynecol J 19: 811–6.
Rubod C, Brieu M, Cosson M, Rivaux G, Clay J, de Landsheere L, Gabriel B. 2012. Biomechanical properties of human pelvic organs. Urology 79: 968–e17.
Rynkevic R, Martins P, Hympanova L, Almeida H, Fernandes A, Deprest J. 2017. Biomechanical and morphological properties of the multiparous ovine vagina and effect of subsequent pregnancy. J Biomech 57: 94–102.
Thornton GM, Shrive NG, Frank CB. 2001. Altering ligament water content affects ligament pre-stress and creep behavior. J Orthop Res 19: 845–51.

Ulrich D, Edwards SI, Su K, White JF, Ramshaw JAM, Jenkin G, Deprest J, Rosamilia A, Werkmeister JA, Gargett CE. 2014a. Influence of reproductive status on tissue composition and biomechanical properties of ovine vagina. PloS One 9: e93172.

Ulrich D, Edwards SL, Letouzey V, Su K, White JF, Rosamilia A, Gargett CE, Werkmeister JA. 2014b. Regional variation in tissue composition and biomechanical properties of post-menopausal ovine and human vagina. PloS One 9: e104972.

Wu JM, Vaughan CP, Goode PS, Redden DT, Burgio KL, Richter HE, Markland AD. 2014. Prevalence and trends of symptomatic pelvic floor disorders in US women. Obstet Gynecol 123: 141.